Iron Antimonate†

Frank J. Berry,* John G. Holden, and Michael H. Loretto
Departments of Chemistry and of Metallurgy and Materials, University of Birmingham, P.O. Box 363, Birmingham B15 2TT
David S. Urch
Department of Chemistry, Queen Mary College, University of London, Mile End Road, London E1 4NS

Iron antimonate, prepared by the calcination of precipitates at elevated temperatures, has been examined by *X*-ray powder diffraction, ^{57}Fe and ^{121}Sb Mössbauer spectroscopy, energy dispersive *X*-ray microanalysis, *X*-ray photoelectron spectroscopy, and Auger electron spectroscopy. The nature of iron antimonate is critically dependent on the environment in which the dried precipitate is calcined. Although iron antimonate prepared from iron-rich reaction mixtures is formed in the presence of α-Fe_2O_3, the iron antimonate prepared by the calcination of equimolar mixtures of iron and antimony and of antimony-rich reactants in air where the excess antimony oxide can volatilise is formed as a rutile-related solid containing iron(III) and antimony(V). Iron antimonate prepared by calcination of antimony-rich reactant mixtures in evacuated sealed silica tubes is covered by a layer of antimony oxide which can be removed by treatment with hydrochloric acid. The rutile-related iron antimonate prepared under these conditions contains iron(III), iron(II), antimony(V), and antimony(III) with the iron(II) species being accommodated in both lattice and surface sites.

Although a material described as iron antimonate was first reported [1] in 1943 during an investigation of rutile-related solids of composition ABO_4, subsequent studies [2–13] have failed to achieve complete unanimity in their descriptions of a material of formula $FeSbO_4$. It appears that whilst there is general agreement that the *X*-ray and neutron diffraction data recorded from iron antimonate are consistent with a material best described in terms of a rutile-related structure containing a random distribution of iron and antimony ions in octahedral sites within the oxygen lattice,[1,4,7,13] the iron-57 and antimony-121 Mössbauer spectra have been interpreted [2–5,8–11] in different ways with some uncertainty persisting over the nature of the cationic oxidation states and confusion as to the origin of magnetic hyperfine interactions. Similarly, studies of the surface properties of iron antimonate, which have frequently been performed during the characterisation of iron–antimony oxide catalysts, have yet to produce a detailed description of the surface regions of the rutile-type solid.[10–11,14–17] Although several of these investigations have involved studies of the nature of surface oxygen,[14–17] some examinations [10,16] by *X*-ray photoelectron spectroscopy have reported that iron antimonate may be enriched at the surface by antimony.

It would seem that the current uncertainty over the fundamental solid-state properties of iron antimonate is, at least partially, a reflection of the different preparative procedures which have been used to synthesise the solid. We have therefore prepared samples of iron antimonate by the calcination of precipitates at elevated temperatures and have investigated the products by a range of techniques. In this paper we describe how the nature of iron antimonate, $FeSbO_4$, is critically dependent on the character and composition of the reactant mixture, and the temperature and environment of the thermal treatment.

Experimental

Iron–antimony oxides, with nominal antimony to iron ratios of 1:5, 1:2, 1:1, 3:1, 5:1, and 10:1 were prepared by adding aqueous ammonia (sp. gr. 0.88) to stirred mixtures of iron(III) nitrate nonahydrate and antimony(V) chloride in nitric acid (sp. gr. 1.42). The precipitates were removed by filtration, washed with water until the washings attained a pH between 6 and 7, dried at 110 °C (18 h) in air, ground, and heated at 500 °C (8 h) in air. The solids were finally calcined at either 1 000 °C (96 h) in air or at 1 000 °C (24 h) in evacuated sealed silica tubes.

X-Ray powder diffraction data were recorded with a Philips PW 1050/70 diffractometer using Cu-K_α radiation and *X*-ray powder diffraction photographs were obtained with a Debye–Scherrer camera using the Straumanis method of film loading.

Mössbauer spectra were recorded with a Cryophysics MS-102 microprocessor-controlled Mössbauer spectrometer. Iron-57 Mössbauer spectra were obtained at 298 K using a $^{57}Co/Rh$ source and absorbers containing *ca.* 10 mg iron cm^{-2}. Antimony-121 Mössbauer spectra were obtained using a $Ca^{121m}SnO_3$ source and absorbers containing *ca.* 10 mg antimony cm^{-2} with both the source and absorber at 77 or 4.2 K. The drive velocity was calibrated with a $^{57}Co/Rh$ source and a natural iron foil absorber. All the spectra were computer fitted, the ^{57}Fe chemical isomer shift data were calculated relative to metallic iron and the ^{121}Sb chemical isomer shifts relative to the calcium stannate source. Transmission electron microscopy and energy dispersive *X*-ray microanalysis (e.d.x.) were performed with a Philips EM400T electron microscope interfaced with an EDAX energy dispersive *X*-ray analysis system.

X-Ray photoelectron spectra (x.p.s.) were recorded with a Vacuum Generators ESCA3 (Mk.1) spectrometer operating at a base pressure of *ca.* 2×10^{-9} Torr using Al-K_α exciting radiation ($h\nu$ = 1 486 eV). The samples were investigated as fine powders mounted on double-sided Sellotape and examined at room temperature. All binding energies were obtained by reference to the C 1*s* binding energy of 285 eV arising from carbon impurity on the sample surfaces.

Auger electron spectra (A.e.s.) were recorded with a Vacuum Generators Fast-scan Auger electron spectrometer operating at 2.5 kV and a base pressure of *ca.* 5×10^{-9} Torr. The samples were examined as fine powders secured on copper mounts by conducting silver paint.

Results and Discussion

The yellow-brown to mid-brown products obtained from the calcination of the dried antimony-rich and equimolar reaction

† *Non-S.I. units employed:* Torr = (101 327/760) Pa, eV ≈ 1.60×10^{-19} J.

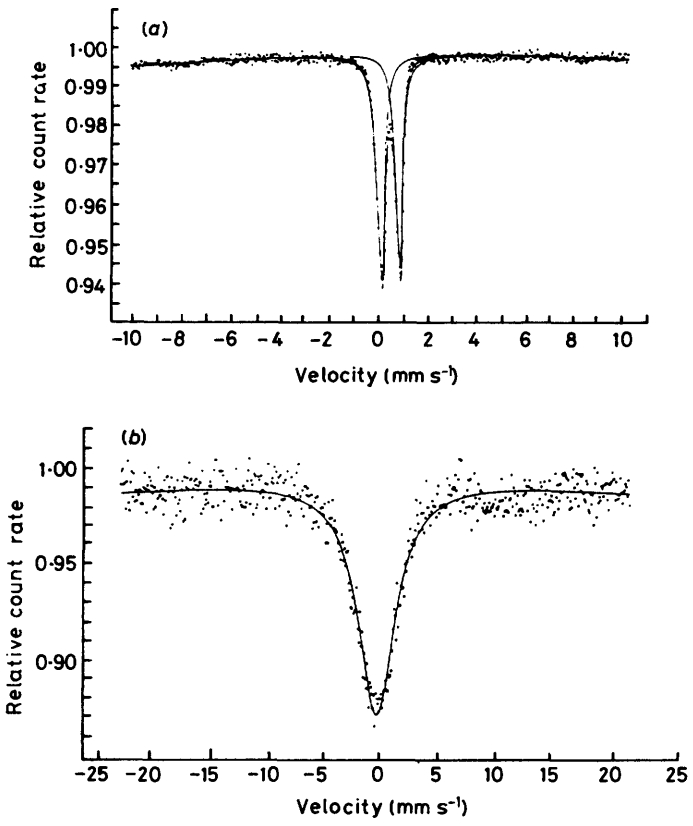

Figure 1. Mössbauer spectra recorded from iron antimonate prepared from a precipitate (Sb:Fe = 5:1) calcined at 1 000 °C (96 h) in air. (*a*) ^{57}Fe Mössbauer spectrum recorded at 298 K. (*b*) ^{121}Sb Mössbauer spectrum recorded at 77 K

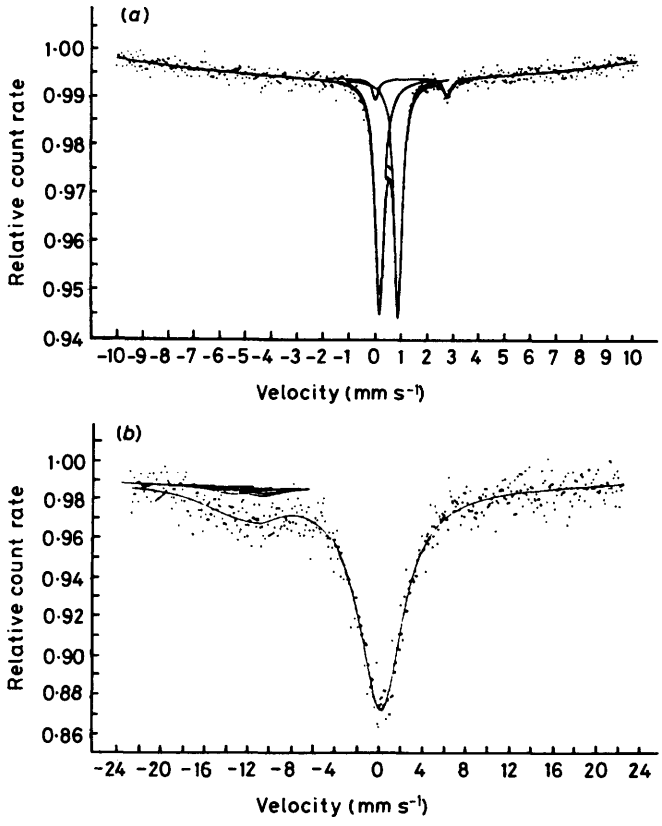

Figure 2. Mössbauer spectra recorded from iron antimonate prepared from a precipitate (Sb:Fe = 5:1) calcined at 1 000 °C (24 h) in an evacuated sealed silica tube. (*a*) ^{57}Fe Mössbauer spectrum recorded at 298 K. (*b*) ^{121}Sb Mössbauer spectrum recorded at 4.2 K

mixtures at 1 000 °C in air gave *X*-ray powder diffraction patterns which were very similar to that previously attributed[7] to monophasic iron antimonate, $FeSbO_4$. The *X*-ray diffraction patterns recorded from the darker brown solids formed from the iron-rich reactants contained additional peaks which could be assigned[18] to α-Fe_2O_3.

The iron-57 Mössbauer spectra recorded from all materials contained a quadrupole split absorption, δ 0.41 ± 0.02 mm s^{-1}, Δ 0.74 ± 0.02 mm s^{-1}, characteristic of high-spin iron(III) [Figure 1(*a*)] and similar to those previously associated[2,3,8,10,11] with iron(III) in $FeSbO_4$. The spectra recorded from the darker brown products also contained a magnetically split pattern, *H* 515 ± 5 kG, characteristic[19] of α-Fe_2O_3. The antimony-121 Mössbauer spectra recorded at 77 K showed [Figure 1(*b*)] a single absorption, δ 0.05 ± 0.05 mm s^{-1}, typical of antimony(V) and similar to those previously reported[2,4,9] for antimony(V) in $FeSbO_4$. Hence the *X*-ray diffraction data and Mössbauer spectra indicate that biphasic products containing $FeSbO_4$ and α-Fe_2O_3 are obtained from iron-rich reactant mixtures. It is also pertinent to note that the presence of the antimony oxide Sb_6O_{13} could be determined in the *X*-ray diffraction patterns recorded from products obtained from antimony-rich reactants after their initial calcination at 500 °C. It would seem that the antimony oxide volatilises when these materials are heated at 1 000 °C in air to form products which give well resolved *X*-ray diffraction patterns and narrow line Mössbauer spectra characteristic of monophasic crystalline iron antimonate containing iron(III) and antimony(V).

The mid-brown products obtained when equimolar or antimony-rich reaction mixtures were calcined at 1 000 °C in an evacuated sealed silica tube also gave *X*-ray powder diffraction patterns characteristic[7] of crystalline monophasic iron antimonate. However, the antimony-rich reaction mixtures gave, in addition to the iron antimonate phase, a highly crystalline opaque solid at a cooler region of the tube which was characterised[20] by *X*-ray powder diffraction as β-Sb_2O_4. This antimony tetraoxide phase presumably arises from the oxidation of the excess antimony when the reaction mixture is heated at 500 °C and its volatilisation and subsequent condensation when calcined in the sealed tube at 1 000 °C.

The mid-brown solids gave ^{57}Fe Mössbauer spectra, composed of a quadrupole split absorption, δ 0.40 ± 0.01 mm s^{-1}, Δ 0.74 ± 0.01 mm s^{-1}, similar to that previously attributed[2,3,8,10,11] to iron(III) in $FeSbO_4$. However, and in contrast to the iron antimonate formed in air at 1 000 °C, the ^{57}Fe Mössbauer spectrum of the iron antimonate formed in sealed silica tubes also showed a quadrupole split absorption, δ 1.18 ± 0.06 mm s^{-1}, Δ 3.16 ± 0.06 mm s^{-1}, characteristic of a high-spin iron(II) species and indicative of *ca.* 5% of the iron being present in the reduced form [Figure 2(*a*)]. The ^{121}Sb Mössbauer spectrum recorded from these solids at 4.2 K showed an absorption, δ 0.28 ± 0.06 mm s^{-1}, characteristic of antimony(V) and similar to that previously reported[2,4,9] for antimony(V) in iron antimonate, and another absorption, δ −12.27 ± 0.06 mm s^{-1}, e^2qQ 17.14 ± 0.10 mm s^{-1}, characteristic of a similar amount, *i.e. ca.* 5%, of antimony(III) [Figure 2(*b*)].

It is important to note that the *X*-ray powder diffraction patterns recorded from the crystalline iron antimonate prepared in the sealed tubes were composed of well defined peaks and gave no evidence for the presence of any other crystalline phases, such as $FeSb_2O_4$ or $FeSb_2O_6$, which might contain the

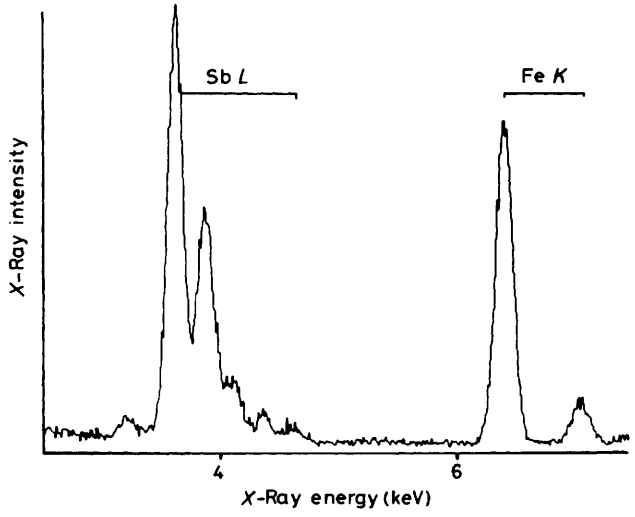

Figure 3. Energy dispersive *X*-ray spectrum recorded from a single particle of iron antimonate prepared at 1 000 °C (24 h) in an evacuated sealed silica tube

iron(II) or antimony(III) species. The possibility that these, or other, phases were present as non-crystalline materials was also eliminated by an examination of the products by transmission electron microscopy which found no evidence for any amorphous material. In this respect it is pertinent to note that energy dispersive *X*-ray microanalysis gave spectra (Figure 3) in which the relative areas of the peaks characteristic of the Sb *L*- and Fe *K*-*X*-rays were indicative of materials composed of approximately equal concentrations of iron and antimony. Given that similar e.d.x. spectra were obtained from the iron antimonate formed by the calcination of precipitates at 1 000 °C in air and that other iron–antimony oxides such as $FeSb_2O_4$ and $FeSb_2O_6$ would be expected to give e.d.x. spectra with antimony to iron ratios of 2:1, the results, taken together, are consistent with the formation in the sealed tubes of another form of iron antimonate containing iron(III), iron(II), antimony(V), and antimony(III), but in which the total iron to total antimony ratio is 1:1.

The iron antimonate containing iron(III) and antimony(V) formed at 1 000 °C in air gave an *X*-ray photoelectron spectrum (Figure 4) in which the Fe $2p_{\frac{3}{2}}$ peak at a binding energy of 714 eV is characteristic[21] of iron(III). Although the presence of oxygen in iron antimonate cannot be directly detected by x.p.s. because of the coincidence[22,23] of the Sb $3d_{\frac{3}{2}}$ and O 1*s* peaks at 531—532 eV, the O $KL_{2,3}L_{2,3}$ Auger electron peak at a binding energy of 976.5 eV confirmed[24,25] the presence of oxygen in the sample. The peaks in the x.p.s. spectrum at 541.2 and 531.5 eV can be ascribed to Sb $3d_{\frac{3}{2}}$ and Sb $3d_{\frac{5}{2}}$ respectively. However, the peaks reveal an anomalously high intensity ratio of *ca.* 1:2.2, as compared with the expected intensity ratio of 1:1.5, and the full width at half height of 1.8 eV of the peak at 541.2 eV is different from the width of 2.2 eV of the peak at 531.5 eV. Both these effects can be associated with the presence of the O 1*s* photoelectron peak beneath the Sb $3d_{\frac{3}{2}}$ peak. Detailed investigations[26–29] of the Sb 3*d* peaks in the x.p.s. spectra recorded from mixed-valence compounds have shown that remarkably small ionisation energy changes of *ca.* 0.5 eV are associated with the oxidation of antimony(III) to antimony(V) and that it is difficult to use the Sb 3*d* chemical shift data to determine the antimony oxidation state with confidence.[30,31] However, small shifts of the Sb 3*d* peaks to lower binding energies can be discerned between the x.p.s. spectrum recorded from the iron antimonate prepared in air

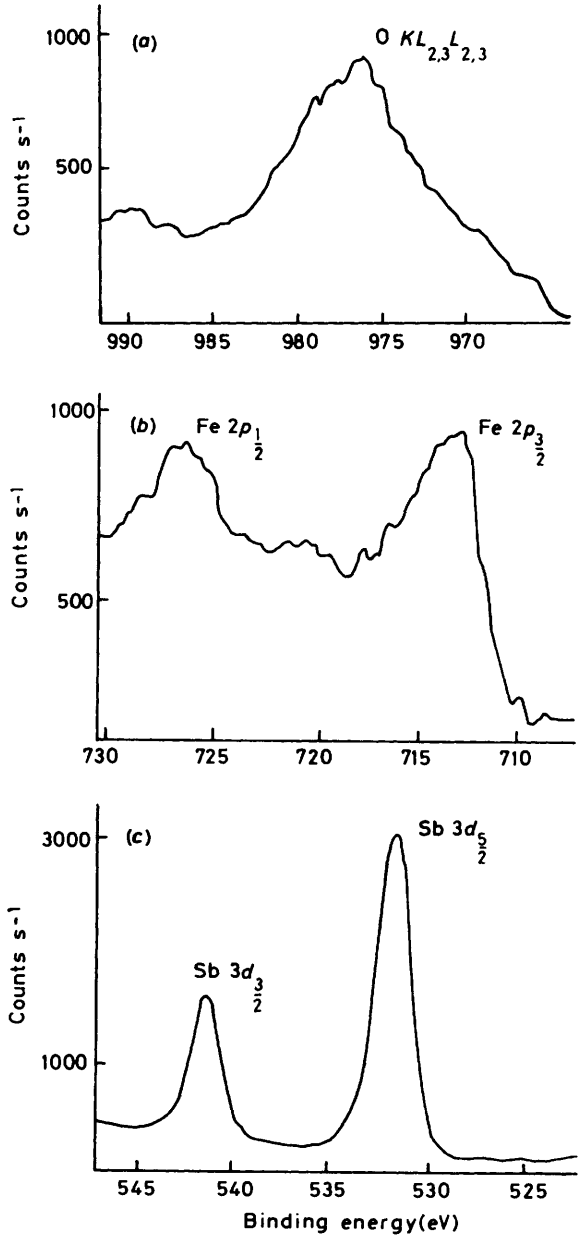

Figure 4. *X*-Ray photoelectron spectrum recorded from iron antimonate prepared at 1 000 °C (96 h) in air: (*a*)—(*c*) are different parts of the spectrum of binding energies scanned

(Figure 4) and that synthesised in a sealed tube under vacuum (Figure 5) which are consistent with the presence of antimony(V) in the former sample and of both antimony(V) and antimony(III) in the latter. The Auger electron spectrum recorded from the iron antimonate prepared at 1 000 °C in air contained signals at 457, 503, and 701 eV characteristic[24] of antimony, oxygen, and iron respectively.

The x.p.s. spectrum recorded from the iron antimonate containing iron(III), iron(II), antimony(V), and antimony(III) which had been prepared in an evacuated sealed tube failed to show a peak corresponding to the Fe 2*p* binding energy (Figure 5) and thereby indicates that the top 50 Å of the surface layer contains less than 5% iron. In this respect it is also relevant to note the greater area of the antimony peak in the A.e.s. spectrum of this solid as compared with that recorded from the iron antimonate prepared in air. Hence the x.p.s. and A.e.s. data recorded from

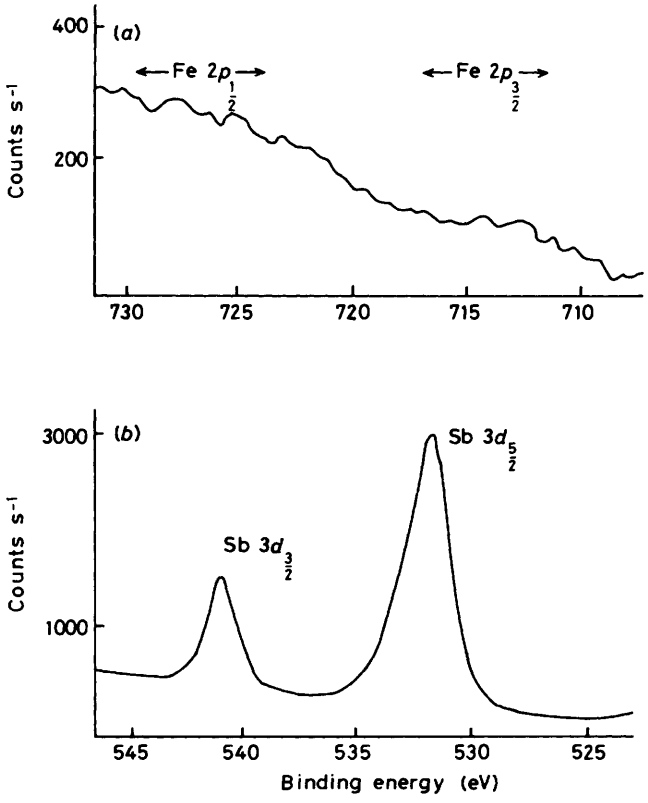

Figure 5. *X*-Ray photoelectron recorded from iron antimonate prepared at 1 000 °C (24 h) in an evacuated sealed silica tube: (*a*), (*b*) are different parts of the spectrum of binding energies scanned

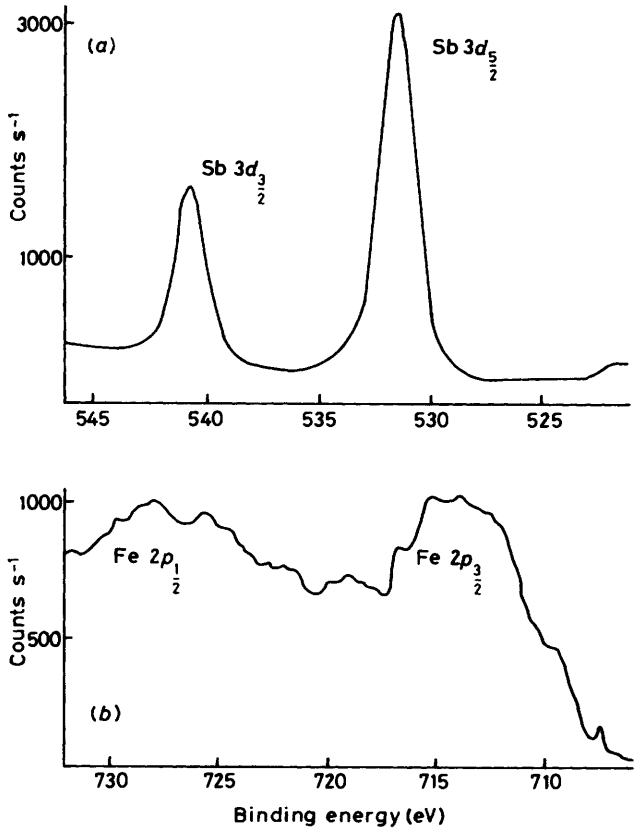

Figure 6. *X*-Ray photoelectron spectrum recorded from iron antimonate prepared at 1 000 °C (24 h) in an evacuated sealed tube and treated with hot concentrated hydrochloric acid: (*a*), (*b*) are different parts of the spectrum of binding energies scanned

the iron antimonate prepared in a sealed tube are indicative of a very high antimony:iron ratio in the surface layers. Despite the normal shape of the Sb $3d_{\frac{3}{2}}$ peak, it is interesting to note the asymmetry and the increase to 2.5 eV in full width at half height of the Sb $3d_{\frac{3}{2}}$ peak. It is also pertinent to note the increase in the Sb $3d_{\frac{3}{2}}$:Sb $3d_{\frac{5}{2}}$ peak height ratio to 1:2.4. Whilst both peaks shift to lower binding energies by *ca.* 0.5 eV as a result of the presence of some antimony(III), see above, the behaviour of the peak at 530—532 eV appears to indicate the presence of additional oxygen in the surface layers. It is possible that the additional oxygen might originate from trace quantities of silica which are deposited on the sample surface during the preparation at 1 000 °C in the sealed silica tube. Although the almost exact overlap of the Si 2*s* and Si 2*p* photoelectron peaks with those of Sb 4*s* and Sb 4*p* precludes confirmation of this hypothesis by x.p.s. it is relevant to note that the O 1*s* peak from the oxygen in silica is observed[32] at 532.5 eV which coincides with the position of the asymmetry of the Sb $3d_{\frac{3}{2}}$ peak in Figure 5. If this explanation of the x.p.s. spectrum is correct then the surface of the iron antimonate prepared at high temperature in sealed silica tubes is composed of an oxide containing both antimony(V) and antimony(III) with some silica contamination.

The enrichment by antimony of the surface of the iron antimonate formed in a sealed tube may be considered as arising from incomplete volatilisation of excess antimony oxide such that a thin layer of antimony oxide, not detectable by *X*-ray diffraction, Mössbauer spectroscopy, or e.d.x., is formed on the surface. Although such a layer could be removed by argon-ion bombardment and the underlying material analysed by x.p.s., it must be acknowledged that such treatment is likely to cause reduction which would compromise any examination of the antimony oxidation states. However, the removal of the surface layer by treatment with hot hydrochloric acid (sp. gr. 1.18) would not give rise to such reduction and a sample prepared in this way gave the x.p.s. spectrum shown in Figure 6. Although the Sb 3*d* peaks have the same form and the same relative intensities as those recorded from the iron antimonate produced at 1 000 °C in air, the peaks are clearly shifted to lower binding energies by *ca.* 0.5 eV. The lower intensities of the iron 2*p* peaks relative to the Sb 3*d* peaks as compared with those recorded from iron antimonate formed in air may reflect the inhibition of some residual superficial antimony oxide to removal. The most significant feature of the x.p.s. spectrum depicted in Figure 6 is the shift in the Fe 2*p* peaks to lower binding energies and the absence of the weak satellite peak at *ca.* 721 eV which is characteristic of iron(III). The results show that the antimony oxide-free surface of iron antimonate formed at 1 000 °C in a sealed tube contains both iron and antimony in reduced oxidation states. Although the quality of the x.p.s. results is not sufficient to determine a precise antimony:iron ratio, the relative magnitudes of the antimony and iron peaks in the Auger electron spectra recorded from the iron antimonate formed at high temperature in air and that prepared in an evacuated sealed tube and treated with hydrochloric acid were very similar. The results are indicative of equal numbers of iron and antimony species in the surface regions of both samples and are inconsistent with the presence of other phases such as $FeSb_2O_4$ or $FeSb_2O_6$ as has been suggested in the past.[16]

Hence the iron antimonate phase formed in an evacuated sealed tube would appear to contain iron(II) as an integral part of the $FeSbO_4$ structure. It is therefore pertinent to note the large Mössbauer quadrupole splitting recorded from the iron(II)

species, Δ 3.16 $\pm$ 0.06 mm s^{-1}, which is characteristic[33] of iron(II) in near-octahedral oxygen co-ordination and which is consistent with the occupation by iron(II), at least partially, of lattice sites. The Mössbauer and x.p.s. data therefore suggest that the iron(II) species exists in the surface regions of $FeSbO_4$ only when iron(II) is also present in the bulk. In this respect it is relevant to note that the lattice parameters of the iron antimonate prepared in air containing iron(III) and antimony(V) which were determined from Debye–Scherrer *X*-ray powder diffraction photographs, $a = b = 4.633\,2(3)$, $c = 3.072\,2(6)$ Å, were smaller than those recorded from the iron antimonate containing iron(III), iron(II), antimony(V), and antimony(III) which was formed in an evacuated sealed tube, $a = b = 4.637\,8(3)$, $c = 3.077\,1(3)$ Å. The results are consistent with the expansion of the lattice resulting from the incorporation of the larger[34] iron(II) species in six-co-ordinate octahedral sites within the rutile-type structure.

Given that antimony(III) is more stable in four-fold co-ordination[35] it is likely that this species is more favourably accommodated in the surface of the rutile-type solid whilst the antimony(V), which prefers[35] six-fold octahedral co-ordination, is accommodated within the bulk rutile-type iron antimonate lattice. Hence we conclude that two types of iron antimonate corresponding to the formulation $FeSbO_4$ can be prepared at high temperatures. Our investigations by convergent beam electron diffraction have shown that, contrary to the previous reports based on *X*-ray and neutron diffraction[1,4,7,13] which have described $FeSbO_4$ as a rutile-related structure containing a random distribution of cations in octahedral sites within the oxygen lattice, the two modifications of iron antimonate described in this work contain superlattices composed of ordered arrays of cations. We shall, in a subsequent report,[36] describe how the cationic ordering in iron antimonate containing iron(III), iron(II), antimony(V), and antimony(III) extends over a longer range than that which occurs in the iron antimonate which contains only iron(III) and antimony(V).

References

1 K. Brandt, *Ark. Kemi Mineral. Geol., Part A*, 1943, **17**, 15.
2 J. B. Wooten, G. G. Long, and L. H. Bowen, *J. Inorg. Nucl. Chem.*, 1974, **36**, 2177.
3 G. M. Bartenev, R. R. Zakirov, and A. D. Tsyganov, *Sov. Phys.-Solid State*, 1975, **16**, 2409.
4 J. D. Donaldson, A. Kjekshus, D. G. Nicholson, and T. Rakke, *Acta Chem. Scand., Ser. A*, 1975, **29**, 803.
5 B. Sh. Galyamov, K. P. Mitrofanov, M. V. Plotnikova, J. T. Folkina, Yu. E. Roginskraya, and Yu. N. Venevtev, *Sov. Phys.-Solid State*, 1977, **19**, 1565.
6 E. Husson, Y. Repelin, and H. Brunet, *J. Solid State Chem.*, 1980, **33**, 375.
7 J. Amador and I. Rasines, *J. Appl. Crystallogr.*, 1981, **14**, 348.
8 M. Petrera, A. Gennaro, N. Burriesci, and J. C. J. Bart, *Z. Anorg. Allg. Chem.*, 1981, **472**, 179.
9 H. Kriegsmann, G. Ohlmann, J. Scheve, and F. J. Ulrich, Proceedings of the Sixth International Congress on Catalysis, eds. G. C. Bond, P. B. Wells, and F. C. Tompkins, The Chemical Society, London, 1976, p. 838.
10 N. Burriesci, F. Garbani, M. Petrera, and G. Petrini, *J. Chem. Soc., Faraday Trans. 1*, 1982, 817.
11 I. Matsuura, Proceedings of the Sixth International Congress on Catalysis, eds. G. C. Bond, P. B. Wells, and F. C. Tompkins, The Chemical Society, London, 1976, p. 819.
12 U. Gakiel and M. Malamud, *Am. Mineral.*, 1969, **54**, 299.
13 R. G. Teller, J. F. Brazdil, R. K. Grasselli, and W. Yelon, *J. Chem. Soc., Faraday Trans. 1*, 1985, 1693.
14 I. Aso, T. Amamoto, N. Yamazoe, and T. Seiyama, *Chem. Lett.*, 1980, **11**, 1435.
15 T. V. Adamiya, Yu A. Mishchenko, D. A. Dublin, and A. I. Gel'bshtien, *Kinet. Katal.*, 1970, **11**, 1168; *Chem. Abstr.*, 1974, **74**, 25527.
16 I. Aso, T. Amamoto, N. Yamozoe, and T. Seiyama, *Chem. Lett.*, 1980, **4**, 365.
17 I. Aso, T. Amamoto, N. Yamozoe, and T. Seiyama, *J. Catal.*, 1980, **64**, 29.
18 ASTM, Index Card No. 24-72.
19 O. C. Kistner and A. W. Sunyar, *Phys. Rev. Lett.*, 1960, **4**, 412.
20 ASTM, Index Card No. 17-620.
21 W. T. Huntress and L. Wilson, *Earth Planet. Sci. Lett.*, 1972, **15**, 59.
22 F. J. Berry, M. E. Brett, R. A. Marbrow, and W. R. Patterson, *J. Chem. Soc., Dalton Trans.*, 1984, 985.
23 L. I. Yin and I. Adler, 'Instrumental Analysis,' eds. H. H. Bauer, G. D. Christian, and J. E. O'Reilly, Allyn and Bacon, Boston, 1978, p. 424.
24 L. E. Davis, N. C. MacDonald, P. W. Palmberg, G. E. Riach, and R. E. Webber, 'Handbook of Auger Electron Spectroscopy,' 2nd edn., Physical Electronics Industries Inc., Minnesota, 1976, pp. 33, 83, 161.
25 T. A. Carlson, 'Photoelectron and Auger Spectroscopy,' Plenum, New York, 1976.
26 A. F. Orchard and G. Thornton, *J. Chem. Soc., Dalton Trans.*, 1977, 1238.
27 P. Burroughs, A. Hamnett, and A. F. Orchard, *J. Chem. Soc., Dalton Trans.*, 1974, 565.
28 M. J. Tricker, I. Adams, and J. M. Thomas, *Inorg. Nucl. Chem. Lett.*, 1972, **8**, 633.
29 T. Birchall, J. A. Connor, and I. H. Hillier, *J. Chem. Soc., Dalton Trans.*, 1975, 2003.
30 Y. M. Cross and D. R. Pyke, *J. Catal.*, 1979, **58**, 61.
31 Y. Boudeville, F. Figueras, M. Forissier, J. L. Portfaix, and J. C. Vedrine, *J. Catal.*, 1979, **58**, 52.
32 T. L. Barr, *Appl. Surf. Sci.*, 1983, **15**, 1.
33 R. Ingalls, *Phys. Rev. A*, 1974, **133**, 787.
34 R. D. Shannon, *Acta Crystallogr., Sect. A*, 1976, **32**, 751.
35 M. B. Robin and P. Day, *Adv. Inorg. Chem. Radiochem.*, 1976, **10**, 247.
36 F. J. Berry, J. G. Holden, and M. H. Loretto, *J. Chem. Soc., Faraday Trans. 1*, 1987, 615.

Received 7th July 1986; *Paper* 6/1349